



Determination of Attenuation and Geometric Damping on Clayey Sand Residual Soil in Irregular Profile using Surface Wave Method

S.A. Rosyidi

Dept. of Civil Engineering, Muhammadiyah University of Yogyakarta, Indonesia

M.R. Taha, Z. Chik, A. Ismail

Dept. of Civil & Structural Engineering, Universiti Kebangsaan Malaysia, Malaysia

Keywords: frequency-independent attenuation, geometric damping, SASW method

ABSTRACT: The spectral analysis of surface wave (SASW) method is a non-destructive testing technique based on the Rayleigh wave dispersion that has been advanced in this study for the evaluation of the material properties of the soil subgrade structure in irregular profile, i.e. pavement system. The Rayleigh wave is generated by transient impact sources and then the wave motion is processed using the spectrum analyzer to obtain the amplitude spectrum of vertical displacement in the frequency domain. The objective of this study is to describe the procedure of the SASW method for determining the frequency-independent attenuation, a_0 and the geometric damping ratio, D of the soil structure. Both parameters are useful for dynamic geotechnical structural design. A frequency-independent attenuation empirical coefficient (a_0) of the Bornitz equation was obtained from the auto power spectrum produced by the spectrum analyzer. Subsequently the damping ratio (D) was able to be calculated using the attenuation coefficient parameter from the Bornitz model. The damping ratio obtained by the Bornitz model was similar to the values calculated using Spectral Ratio and Transfer Function model. Good agreement was also found between the values obtained in this study compared to that of other researchers.

1 Introduction

Many problems related to soil dynamics require the knowledge of the attenuation of seismic wave propagation in the ground. For geotechnical and pavement structures, wave attenuation is useful for determining the effects of vibration on the affected area. The attenuations of waves are determined from the radiation and material damping of the structure. The damping ratio is also an important parameter which measures the dynamic response of a system at resonance (Clough and Penzien, 1993), ground amplification during earthquake (Vucetic and Dobry, 1991) and enhancement of reservoir characterization (Klimentos, 1995). Many in situ and laboratory tests have been used to evaluate damping ratio. Many studies have been also conducted to obtain the damping behavior and empirical correlations between the damping ratio in terms of attenuation and the amount of radiated energy compared to the frequency of vibration and type of soil. Lai (1998), Rix & Lai (1998), and Rix et al. (2000) employed surface wave measurements to determine the material damping ratio profile of a layered soil deposit. In their studies, an attenuation curve was constructed from the observed spatial attenuation of Rayleigh wave amplitudes and then was inverted to obtain the material shear damping ratio. The analytical procedures which they used to obtain the shear wave velocity and damping ratio profile were performed separately. However, studies on the relationships between the damping ratio obtained from in situ measurements of seismic wave attenuation and the stiffness of soil subgrade of pavement structure were relatively few.

The aim of this paper is to determine the frequency-independent attenuation coefficient (α_0) and the damping ratio (D) of the generated Rayleigh wave (R-wave) on the soil subgrade structure using the spectral analysis of surface wave (SASW) method. The SASW method is an in situ seismic technique originally used to evaluate the stiffness of pavement layers at low strains. The method is based on the dispersion phenomena of R-waves in layered media. This study is also conducted to show the capability of the SASW method for attenuation measurement of clayey sand residual soil layer in irregular profile of a pavement structure.

2 Soil Attenuation and Damping Ratio

Attenuation in soil dynamics is a phenomenon that involves the interaction of several mechanisms that contributed to the energy dissipation of the seismic wave during dynamic excitation (Rix et al., 2000) while material damping is caused by the energy dissipated within the soil skeletal frame. The physical mechanism that has been postulated to be responsible for material damping is the energy loss in materials, for instance, the frictional losses between soil particles (White 1983). The damping ratio (D) is defined as the ratio between the energy loss and a maximum stored energy within one loading-cycle (Figure 1). Under the low-loss condition, the relationship between quantities used in different disciplines to characterize fundamental attenuation and material damping follows:

$$Q^{-1} = 2D = \frac{DE}{2pE} \quad (1)$$

where Q^{-1} is the dissipation factor which describes as material attenuation, DE energy dissipated during one cycle at circular frequency ω and E the maximum strain energy stored during referred cycle.

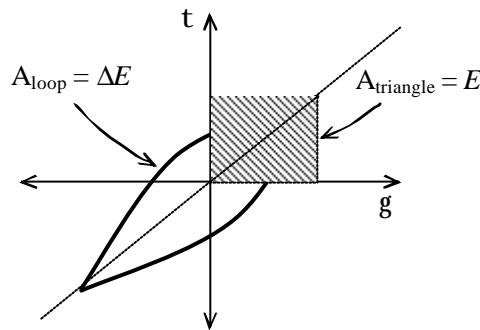


Figure 1. Damping obtained from the cyclic shear stress – strain curve.

Aki & Richards (1980) mentioned that D behaved as frequency independent for $0.1 < f < 10$ Hz which is also called hysteretic or rate-independent damping. Material damping can also be obtained using the attenuation coefficient (α) and the logarithmic decrement (δ) in which their relationship is written as:

$$D = \frac{\alpha c}{2p} = \frac{d}{2p} \frac{1}{\sqrt{1 + \left(\frac{d}{2p}\right)^2}} \quad (2)$$

where c is seismic wave velocity. The damping ratio during dynamic excitation is usually a small value (less than 10 %), consequently the second order terms are negligible and equation (2) can be rewritten as:

$$D = \frac{\alpha c}{2p} = \frac{d}{2p} \quad (3)$$

Other physical mechanisms also contributed to the decay in the seismic wave amplitude that propagates in the soil mass. The first mechanism is the spreading of energy over an expanding area as the wavefront propagates away from the source causing the amplitude of waves to attenuate with increasing distance from the source (geometric or radiation damping). The second mechanism explained that the reflection and transmission of seismic waves at inter-faces, mode conversions and scattering in non homogeneous media causes the wave amplitude to diminish (Rix et al., 2000).

3 Research Methods

3.1 Spectral Analysis of Surface Wave (SASW) Method

Two key elements of the SASW method are the generation of surface wave energy from impact sources and the measurement of the particle motion of the R-wave at suitable distances from the source on the surface of

media. In layered soil media, the surface wave velocity depends on the frequency (or wavelength) of the wave. The variation of the velocity with frequency is called dispersion and arises due to the different wavelengths of waves passing through the layered media. Short wavelengths (high frequency) of waves propagate only through near-surface materials while longer wavelengths (lower frequency) of waves propagate in deeper layers. A plot of surface (R-) wave velocity versus frequency is called the dispersion curve.

The experimental set up of the SASW test is shown in Figure 2(a). R-waves in field tests were detected using two receivers (piezoelectric accelerometers) for post processing. Several configurations of the accelerometers (d_2) and the source (d_1) spacings were required in order to sample different depths. Short receiver spacings (5 and 10 cm) of high frequency (short wavelengths) were used to sample the pavement surface layer while larger receiver spacings (40 and 160 cm) of low frequency (long wavelengths) were implemented to sample the pavement base and subgrade layers. The arrangement of receivers which was adopted in this study is the common receivers midpoint geometry. This arrangement is illustrated in Figure 2(b). The SASW test was carried out at 40 different sites on a road inside the Universiti Kebangsaan Malaysia campus in Bangi, Malaysia.

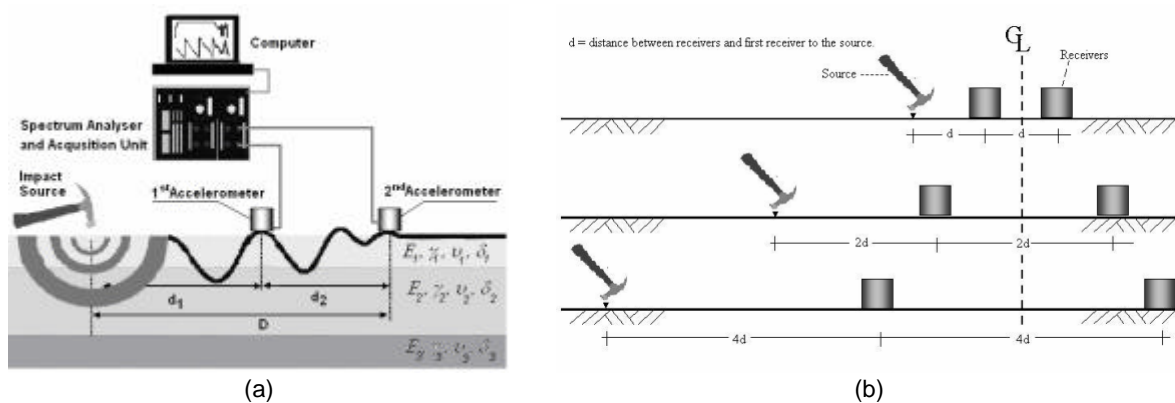


Figure 2. Field set up of SASW measurement (a) and its arrangement of receivers (b)

The signals produced from impact sources in time domain are digitalised and recorded in time domain by a dynamic spectral analyser. Consequently, they are transferred into its frequency domain and displayed into several spectrum functions such as the transfer function, coherence and auto power spectrum. Subsequently, the experimental dispersion curve of the phase velocity and wavelength were developed from the phase information of the transfer function at the frequency range satisfying the coherence criterion. The time of travel between the receivers for each frequency can be calculated by:

$$t(f) = \frac{f(f)}{360f} \quad (4)$$

where f is the frequency; $t(f)$ and $f(f)$ are respectively the travel time and the phase difference in degrees at a given frequency. The distance of the receiver (d) is a known parameter. Therefore, the R-wave velocity, V_R or the phase velocity at a given frequency is simply obtained by:

$$V_R = \frac{d}{t(f)} \quad (5)$$

and the corresponding wavelength of the R-wave, L_R may be written as:

$$L_R(f) = \frac{V_R(f)}{f} \quad (6)$$

The actual shear wave velocity of the layered profile is produced from the inversion of the composite experimental dispersion curve. The inversion is employed using several modeling approaches available for SASW applications. Among them are the transfer matrix method (Haskell, 1953), the dynamic stiffness matrix method (Kausel and Rössset, 1981), and the finite difference method (Hossain and Drnevich, 1989). In this inversion process, a profile of a set of a homogeneous layer such as pavement surface, base, subbase and subgrade layer, extending to infinity in the horizontal direction was assumed. The last layer is usually taken as a homogeneous half-space. Based on the initial profile, a theoretical dispersion curve was constructed using an automated forward modeling analysis of the 3-D dynamic stiffness matrix method (Kausel and Rössset, 1981). The theoretical dispersion curve was ultimately matched to the experimental dispersion curve based

on lowest root mean square (RMS) error with an optimization technique from software of WinSASW (Joh, 1996; Rosyidi, 2004)

In order to measure the attenuation and geometric damping ratio from signal spectrums recorded from SASW test, the Bornitz model was employed in the analysis. The decrease in amplitude (energy density) of the vertical component of the R-wave with distance due only to geometric configuration is also called the radiation damping or geometric spreading which is expressed by:

$$w_2 = w_1 \left(\frac{r_1}{r_2} \right)^n \quad (7)$$

where w_1 is the amplitude of vibration at distance r_1 from the source, w_2 the amplitude at distance r_2 from the source and n the attenuation factor due to radiation damping which depends on the type of seismic wave, the position and size of the seismic source (Table 1).

Table 1. Attenuation radiation damping factor (n) with the source on the surface (Kim and Lee, 1998)

Source Type	Induced Wave	n
Point	Body Wave	2.0
	Surface Wave	0.5
Infinite line	Body Wave	1
	Surface Wave	0

The vibration energy of the R-wave is also dissipated during its propagation by the material damping which is also described by the damping ratio (D). An effective damping ratio of R-wave in layered medium can be defined and the value is frequency dependent. Its value may become very high for the first few modes of vibration.

There are several models to describe the combined effect of both the radiation and material damping. The Bornitz equation is one of the common models used and can be described by:

$$w_2 = w_1 \left(\frac{r_1}{r_2} \right)^n e^{-a(r_1-r_2)} \quad (8)$$

where a is the attenuation coefficient of the material (m^{-1}).

The attenuation coefficient of material depends on the type of material and the frequency of vibration. The estimated value of the attenuation coefficient can be obtained using the R-wave velocity (V_R), the frequency of vibration (f) and the damping ratio (D) using the following equation:

$$a = \frac{2pD}{V_R} \quad (9)$$

From the above relationship, the attenuation coefficient linearly increases with the vibration frequency and is inversely proportional with the R-wave velocity.

Alternatively, the independent-frequency attenuation coefficient (Athanasopoulos et al., 2000) can be obtained by writing Equation 9 in the form:

$$a_0 = \frac{a}{f} = \frac{2pD}{V_R} \quad (10)$$

where a_0 is the frequency-independent of attenuation coefficient in unit of s/m.

3.2 Spectral Ratio Method for Damping Ratio

The spectral ratio method has been utilized to determine the in-situ intrinsic attenuation of seismic waves (Campanella et al., 1994). The damping ratio obtained using spectral ratio method can be expressed as (Wang et al., 2004):

$$\ln \left(\frac{A_1(f)}{A_2(f)} \right) = -\ln \left(\frac{C_1}{C_2} \right) - \ln \left[\left(\frac{r_1}{r_2} \right)^n \cdot T \right] + \frac{2pD}{V_R} \cdot (r_2 - r_1) \cdot f \quad (11)$$

where A_1 and A_2 is the Fourier amplitudes for different frequency (f), C_1 and C_2 respectively represents the frequency-independent coupling coefficient and transducer response, D the damping ratio, T transmission coefficient and n the attenuation factor.

From Equation 11, the attenuation due to geometric spreading, reflection and coupling effects are included to the intercept in Equation 11, and does not influence the inferred material damping ratio as long as the parameter of D , V_R and T are assumed to be frequency independent (Wang et al., 2004). Hence, the damping ratio is derived from the double differentiation of Equation 11 as:

$$D = \frac{\partial^2}{\partial r \cdot \partial f} \left(\frac{A_1(f)}{A_2(f)} \right) \cdot \frac{V_R}{2p} \quad (12)$$

3.3 Surface Wave Transfer Function Method for Damping Ratio

Experimental attenuation curves can be simultaneously determined using a single set of multi-channels measurement of phase velocity with transfer function method and dispersion curves as well (Rix et al. 2001). The simultaneous determination provides more consistent and effective result for obtaining material damping ratio (Lai, 1998). The experimental transfer function method for determining damping ratio is implemented by the concept of deconvolution to an ensemble of surface seismic traces with no need for the characterization of the seismic sources. Deconvolution of a signal $f_2(t)$ with a signal $f_1(t)$ is represented in the frequency domain as the ratio between the Fourier transform of the two signals $F_2(\omega)$ and $F_1(\omega)$ respectively:

$$F_{21}(\mathbf{w}) = \frac{F_2(\mathbf{w})}{F_1(\mathbf{w})} = \frac{F_2(\mathbf{w}) \cdot \overline{F_1(\mathbf{w})}}{|F_1(\mathbf{w})|^2} \quad (13)$$

where \mathbf{w} is the circular frequency and F_{21} is equivalent to the transfer function of the system (Foti 2003). Considering a set of multi-channel measurements of particle velocity along a straight line on the ground surface, the experimental transfer function $\tilde{F}(r, \mathbf{w})$ can be estimated using deconvolution of the whole ensemble of signals:

$$\tilde{F}(r, \mathbf{w}) = F_{li}(\mathbf{w}) = \frac{F_i(\mathbf{w})}{F_l(\mathbf{w})} \quad (14)$$

where $F_i(\mathbf{w})$ is the Fourier transform of the i th signal detected at distance r from the sources, $F_l(\mathbf{w})$ the Fourier transform of the signal detected by the closest receiver and $F_l(\mathbf{w})$ the represents the i th deconvolution signal.

The experimental transfer function is then used in regression analysis to estimate the attenuation curves of the surface waves. The analytical expression of the transfer function is obtained from the modeling of soil structures of linear viscoelastic homogeneous layers where the expression is used for regression. By inserting an expression of the complex phase angle, $\psi(r, \mathbf{w})$ which is assumed as $K(\mathbf{w}) \cdot r$ and geometric spread function, $G(r, \mathbf{w})$, Equation (14) can be expressed as (Lai, 1998):

$$\tilde{F}(r, \mathbf{w}) = \frac{G(r, \mathbf{w})}{G(r_1, \mathbf{w})} e^{-i \cdot K(\mathbf{w})(r-r_1)} \quad (15)$$

where $K(\mathbf{w}) = \{[\mathbf{w}/V_R(\mathbf{w})] + i\mathbf{a}_R(\mathbf{w})\}$ is a complex wave number with $V_R(\mathbf{w})$, the phase velocity and $\mathbf{a}_R(\mathbf{w})$, the attenuation coefficient of Rayleigh waves. The assumption $\psi(r, \mathbf{w}) = K(\mathbf{w}) \cdot r$ is equivalent to considering the phase angle $\psi(r, \mathbf{w})$ to be the result of a single mode of surface wave propagation (Rix et al. 2001).

Equation 15 is used in non linear regression analysis to estimate the complex valued wave number $K(\mathbf{w})$ from the experimental values of the transfer function. The experimental complex wave number obtained with the regression procedures contains the information related to surface wave attenuation. It can be used in a complex valued inversion procedure to estimate the damping ratio profiles. Detail discussion for this section can be referred to Rix and Lai (1998) and Foti (2003).

4 Results and Discussion

4.1 Soil Subgrade Layer Properties

The average road-pavement profile consists of an asphalt layer (70 mm thick) and a base of crushed aggregate (400 mm thick) over a soil subgrade. Layer properties and thickness of the three layers are shown in Figure 3. Based on the phase data in transfer function spectrum, the experimental dispersion curve for subgrade layer could be obtained and the result is illustrated in Figure 3. The shear wave velocity was obtained by inversion of the R-wave velocity dispersion curve from SASW measurement. An example of the

final shear wave profile at test site is described in Figure 4. The pavement structure profile in Figure 3 shows that the shear wave velocity gradually decreases with depth. The shear wave velocity of the asphaltic layer was found to be 840 m/s while the base and subgrade layers were 297 m/s and 126 m/s, respectively. The average of the inverted shear wave velocity of the soil subgrade layer for the UKM test sites was found to be 178.689 m/s with a range of 116.44 to 263.226 m/s. Using the shear wave velocity parameter, the soil material of subgrade layer in this study was evaluated and classified as a sandy soil following on Puri (1969) and Nazarian and Stokoe (1986).

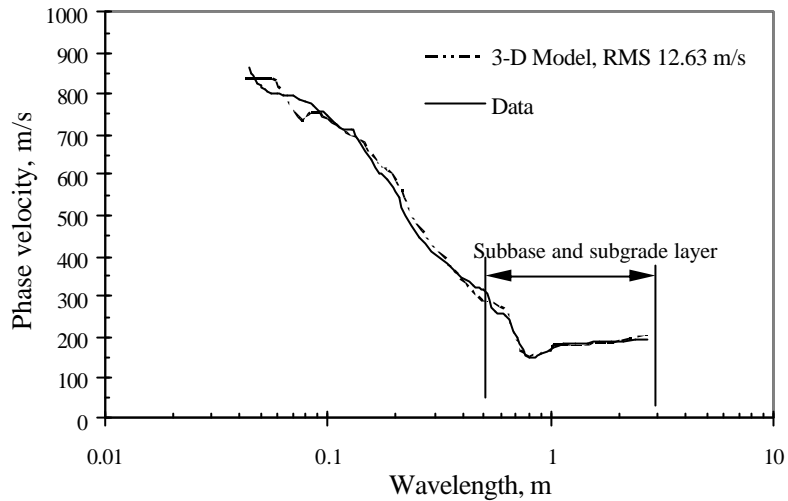


Figure 3. The experimental dispersion curve and the 3-D theoretical curve for phase data of subgrade measurement from 320 cm receiver spacing.

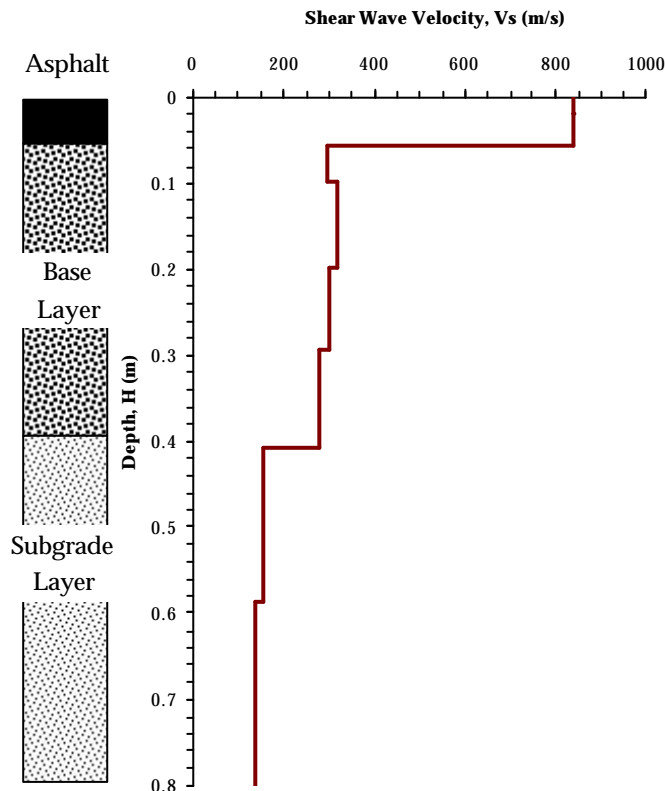


Figure 4. The shear wave velocity profile from the SASW inversion.

Kabir (2005) studied the basic properties of soil subgrade at UKM campus. The basic properties of the soil subgrade at the UKM campus are described in Table 2. From geological studies, the subgrade soil was grouped as meta-sedimentary residual soil. Based on the soil tests using BS 1377:1990, the soil subgrade was classified to sedimentary residual soil with code of SC (clayey sand) or clayed sand residual soil. The result shows that the soil classification based on the shear wave velocities is reasonably in agreement with the laboratory soil properties obtained by Kabir (2005).

Table 2. Soil properties of the subgrade layer

Property	Units		
	%	mm	No Unit
Specific gravity	-	-	2.60
Sand fraction	59	2 – 0.063	-
Silt fraction	18	0.063 – 0.002	-
Clay fraction	23	< 0.002	-
LL	36	-	-
PL	17	-	-
PI	19	-	-
Organic content	0.63	-	-
pH	-	-	4.95

4.2 Attenuation Coefficient in Soil Subgrade Layer

The particle displacement spectra of signals recorded from first and second accelerometer at test sites for $r = 160$ and 320 cm, are illustrated in Figure 5. In this spectrum, the particle displacement may reflect the combination of several mode of Rayleigh wave propagation because the R-waves propagated in a layered media with extreme stiffness contrast.

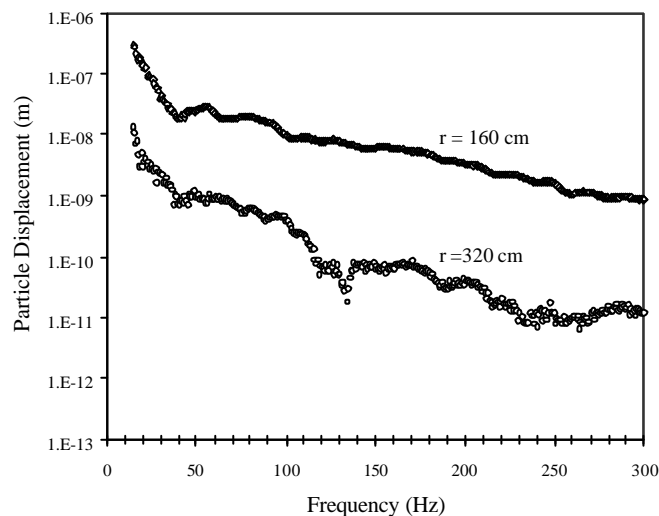


Figure 5. Particle displacement spectra from SASW measurement at selected road site

Figure 6a shows the auto power spectrum from FFT analysis of particle displacement spectra of 160 cm receiver spacing for pavement subgrade assessment. Using the bandwidth criteria, the useful frequency of the signal needed is obtained from the auto power spectra in the range of 68.75 to 135.16 Hz. This frequency range of waves is the effective measured R-waves that propagate in the soil subgrade layer. The plot of the coherence function spectrum (Figure 6b) also indicate that the two signals are highly correlated (coherence magnitude > 0.98) in that frequency range. The use of the coherence function is more useful for goodness level confirmation of the measured frequency from the bandwidth criteria for the subgrade layer.

The decay factor curve of the R-wave for the experimental data is then obtained from the plot of the ratio of the second amplitude (w_2) over the first amplitude (w_1) versus frequency (Figure 7) where the curve shows a

general trend of frequency dependency. A regression analysis is then performed on the experimental data to obtain the decay factor. The Bornitz equation (Equation 10) can then be written as:

$$\frac{w_2}{w_1} = \left(\frac{1}{2}\right)^{0.5} e^{-1.6a_0 f} \quad (16)$$

For a 160 cm receiver spacing, the value of r_1 and r_2 are 1.6 and 3.2 m, respectively. The best-fit curve is then established between the decay factor of the experimental data and the Bornitz equation by trial and error for different values of α_0 from visual best-fit evaluation of the two curves. From Figure 7, the value of frequency-independent attenuation coefficient of the soil subgrade layer of the pavement structure obtained is calculated as 1.9375×10^{-3} s/m. The results of frequency-independent attenuation and the frequency range of each layer of the pavement structure are described in Table 3. The frequency range of the attenuation coefficient of the R-waves in the pavement layers was chosen using the bandwidth criteria.

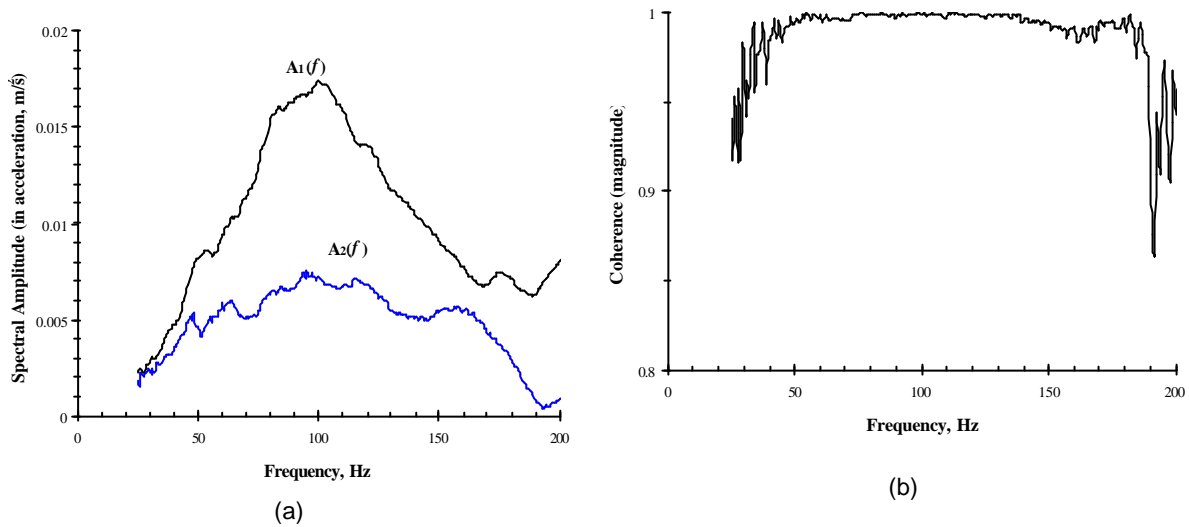


Figure 6. (a) The power spectrum of received signal at first and second receiver, (b) the coherence function spectrum from 160 cm receiver spacing.

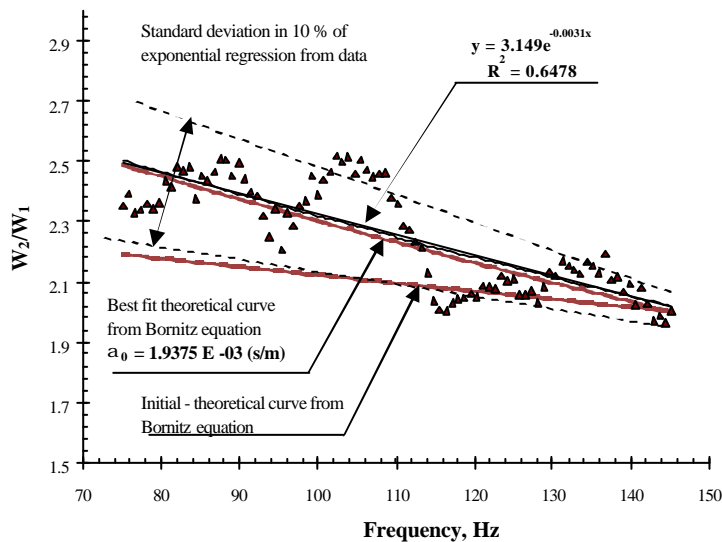


Figure 7. The decay factor curve of amplitude ratio versus frequency of 160 cm receiver spacing for soil subgrade layer.

Table 3. The results of frequency-independent attenuation and the frequency range of each layer

Layer	α_0 ($\times 10^{-3}$ s/m)	COV (%)	Frequency Range (Hz)
Surface	0.432 – 0.653 (average 0.54)	15.6	8 – 13 k
Base	0.883 – 1.012 (average 0.90)	25.7	900 – 1.5 k
Subgrade	1.018 – 2.145 (average 1.58)	22.4	20 - 180

From the results it can be observed that the asphaltic layer has a lower average value of attenuation than the base and subgrade layers. It also indicates that the attenuation increases but material stiffness decreases with depth.

The values of the frequency-independent attenuation coefficient obtained from this study were compared with experimental results that have been carried out by other researchers, such as Yang (1995), Woods (1997), and Athanasopoulos et al. (2000) as shown in Figure 8. Woods and Jedele (1985), and Woods (1997) classified soil groups from the frequency-dependent attenuation of the 5 Hz vibration. The average attenuation coefficient of the subgrade material is 1.58×10^{-3} s/m, i.e. ranging between $1.018 - 2.145 \times 10^{-3}$ s/m. The result falls into Class 1 (soft soil) and Class 2 (medium soil) using Woods (1997) classification. In general, the results are also in good agreement with Athanasopoulos et al. (2000).

Yang (1995) also studied the frequency-independent attenuation coefficient for soil ranging from loose sand and soft clays to rock. Figure 8 shows that the average of this study is close to the lower bound of the attenuation coefficient range obtained by Yang (1995) for unsaturated loose sand material which is most likely due to the difference in material. However, the attenuation coefficient of subgrade material obtained in this study is still within the upper and lower bound of the Athanasopoulos's (2000) empirical correlation of:

$$a_0 = 3.17 \times 10^{-3} \times e^{-\frac{V_s}{500}} \text{ (best-fit)} \quad (17)$$

$$a_0 = 1.15 \times 10^{-3} \times e^{-\frac{V_s}{500}} \text{ (lower bound)} \quad (18)$$

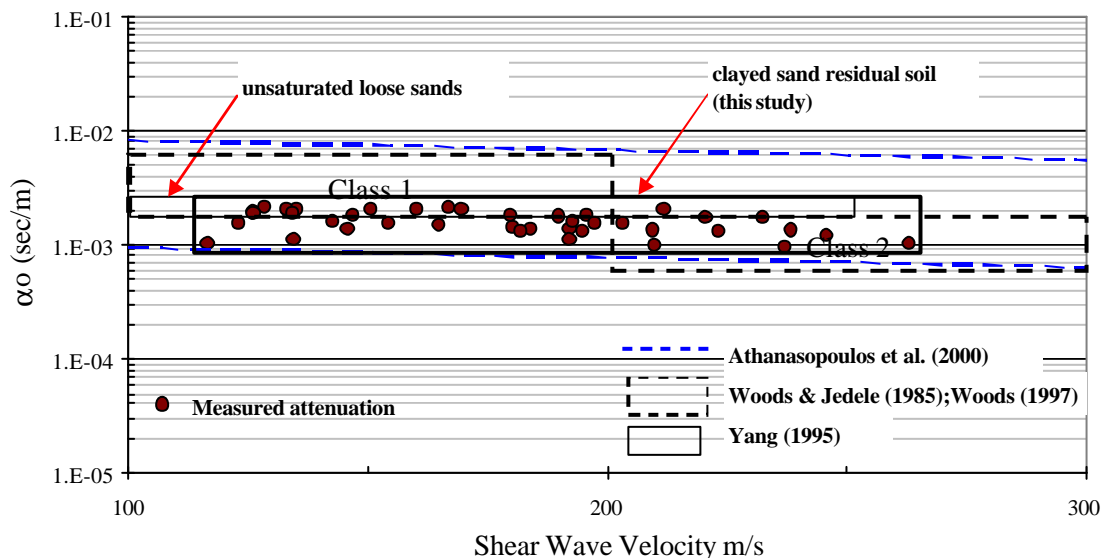


Figure 8. The decay factor curve of amplitude ratio versus frequency of 160 cm receiver spacing for soil subgrade layer.

